

RESEARCH ARTICLE | JANUARY 10 2019

A novel short-term blood pressure prediction model based on LSTM **FREE**

Qingxiang Zhao; Xiaobing Hu ; Jing Lin; Xi Deng; Hang Li

 Check for updates

AIP Conf. Proc. 2058, 020003 (2019)

<https://doi.org/10.1063/1.5085516>


View
Online


Export
Citation

CrossMark

Articles You May Be Interested In

A comparative study of LSTM, Bi-LSTM, and DBi-LSTM network model in forecasting COVID-19 new cases and new deaths in Indonesia

AIP Conference Proceedings (May 2023)

LSTM based flood prediction system

AIP Conference Proceedings (March 2022)

Forecasting energy consumption using enhanced LSTM

AIP Conference Proceedings (November 2022)

500 kHz or 8.5 GHz?
And all the ranges in between.

Lock-in Amplifiers for your periodic signal measurements



Find out more

 Zurich
Instruments

A Novel Short-Term Blood Pressure Prediction Model Based on LSTM

Qingxiang Zhao^{1, a)}, Xiaobing Hu^{1, b)}, Jing Lin^{2, c)}, Xi Deng^{1, d)}, Hang Li^{1, e)}

¹*School of Manufacturing Science and Engineering, Sichuan University, Chengdu 610065, China.*

²*Anesthesiology Department of West China of Medicine/West China Hospital, Sichuan University, Chengdu 610065, China.*

^{a)}scdy_zqx@163.com

^{b)}Corresponding author email: huxb@scu.edu.cn

^{c)}linjingwch@qq.com

^{d)}1459145424@qq.com

^{e)}396511990@qq.com

Abstract. Blood pressure (BP) can reflect many physiological characteristics, and timely monitoring of it can somehow prevent hypertension, asphyxia and other diseases. With the development of clinical medical technology, the accuracy requirements of the intelligent physiological monitoring equipment for predicting the physiological characteristics of BP are gradually increasing. This paper proposes a BP prediction model based on Long Short Term Memory Networks (LSTM-NN), which makes full use of the efficient processing characteristics of LSTM for time series information and accurately predicts the systolic BP and diastolic BP. The primitive photoplethysmographic pulse wave (PPW) signal and actual BP data in different time periods and different states were collected on 6 adult goats simultaneously. The blood flow changes were stimulated by injection of adrenaline to obtain a wide range of raw data to improve the generalization ability of the model. The clinical features of each PPW cycle were introduced into the LSTM model for training and prediction to resolve actual systolic BP and diastolic BP. Comparing the model with the prediction effect of BP neural network (BP-NN) model, the result shows that the prediction accuracy of LSTM model is high and the robustness is strong. The maximum error values for systolic and diastolic pressure prediction are 1.05mmHg and 1.8mmHg, respectively.

Key words: Blood pressure prediction; photoplethysmographic pulse-wave characteristics; LSTM-NN; Time series.

INTRODUCTION

BP is comprised of arterial pressure, venous pressure and capillary pressure according to the different types of vessels, which is generated by the force exerted on the lateral of the vessels wall when blood flows through. The arterial pressure really matters in medical research, for it helps to prevent and diagnose the diseases like Hypertension, diabetes, asphyxia, etc. Traditionally, the measurement methods for BP are divided into invasive and noninvasive two categories, with the development of intelligent sensing technology, modern medicine strives to monitor the BP of patients continuously and dynamically to benefit diagnosis and prevention of related diseases. Literature [1] has shown that dynamic BP monitoring helps in the treatment of hypertension and in assessing target organ damage timely. The Chinese Hypertension League [2] also pointed out that dynamic BP monitoring can improve the accuracy of the diagnosis of hypertension and evaluate the therapeutic effect.

A large number of scholars have done valuable achievements on clinical BP prediction. Zhang Jinghui et al [3] used Backward Propagation Neural Networks (BP-NN) to predict left ventricular BP based on body surface sound characteristics. Enric Monte-Moreno measured BP and blood glucose by extracting the characteristics of photoplethysmographic pulse and using random forest method [4]. Qi Shihua et al [5] made some regression analysis

on characteristic parameters of pulse wave and actual BP; Zhao Yanfeng et al [6] used the Partial Least Squares method to predict the BP with the data consisting of pulse wave transit time and its characteristic parameters.

With the application of innovative technology like Deep Learning and Big Data implanted on intelligent sensing technology, it provides a novel idea for the development of measurement and control technology. This paper focuses on the relationship between blood pressure which is changing continuously and physiological characteristics, body state (such as before and after exercise, before and after catering), and utilized LSTM to train and predict the BP. At present, LSTM has made outstanding contributions in the fields like stock forecasting, speech recognition and translation, intelligent transportation. Shu Fan et al [7] used LSTM to effectively identify low-resource speech; Wang Xiangxue et al. predicted short traffic flow based on LSTM_RNN; besides, LSTM also contributes to efficient prediction of short-term power load [8]; Frank P.-W. Lo et al. developed a system for continuously predicting diastolic and systolic blood pressure[9] using LSTM-NN, but this method requires the pulse wave transit time PTT, which may be inconvenient to get.

Considering the strong periodicity of BP data, this paper explores the characteristic parameters of PPW signals, and studied the correlation between various parameters and systolic blood pressure (SBP) and diastolic blood pressure (DBP). The relevant characteristics playing a role of the input of the LSTM-NN have been filtered. The PPW signals of 6 goats at different times and in different states were collected, and the corresponding SBP and DBP were monitored by invasive measurement simultaneously. The data is reliable and the generalization ability of the wide range model is strong. Compared with the traditional BP-NN, the accuracy of BP prediction has been improved.

DATA COLLECTION AND CHARACTERISTICS EXTRACTION

Animal Experiment

PPW signals data of 6 healthy goats in different state was sampled respectively, and the actual BP signals data of femoral artery was collected simultaneously by BL-420S Bio-signal Acquisition and Analysis System of Taimeng Co.Ltd, with both of whose sampling frequency was 100HZ satisfying Shannon sampling theorem. Three of the goats were intravenously injected with phenylephrine 5-10 ug/kg to accelerate blood flow, the details of them are displayed in Table 1, and a wide range of BP data was obtained to make the model more general. Finally 25450 BP data ranging from 52.16mmHg to 132.39mmHg has been collected in total.

Raw Data Preprocessing and Characteristics Extraction

Filter Processing

There might be some noise signals when sampling, so it is critical to filter the high-frequency or low-frequency noise originated from the factors like goat's respiration, muscle contraction, human operation, and cable. The normal heart rate of goat is generally 70-80 beats per minute (bpm), which is roughly 70-130 bpm after injection of phenylephrine. We filtered the raw PPW signal by setting a 0.2-30HZ pass-band. The original signal is smoothed based on the linear phase of FIR filter. Parts of the time-domain signal before and after filtering is shown in Figure 1. And all the data filtered would be divided as cycle for extracting characteristics.

TABLE 1. Details of 6 adult goats in experiments

| Number | Weight (kg) | Age (months) | Whether to be injected |
|--------|----------------|-----------------|---------------------------|
| 1 | 30.6 | 45 | Yes |
| 2 | 32.6 | 58 | No |
| 3 | 34.3 | 52 | Yes |
| 4 | 38.6 | 48 | No |
| 5 | 39.5 | 60 | Yes |
| 6 | 40.2 | 62 | No |

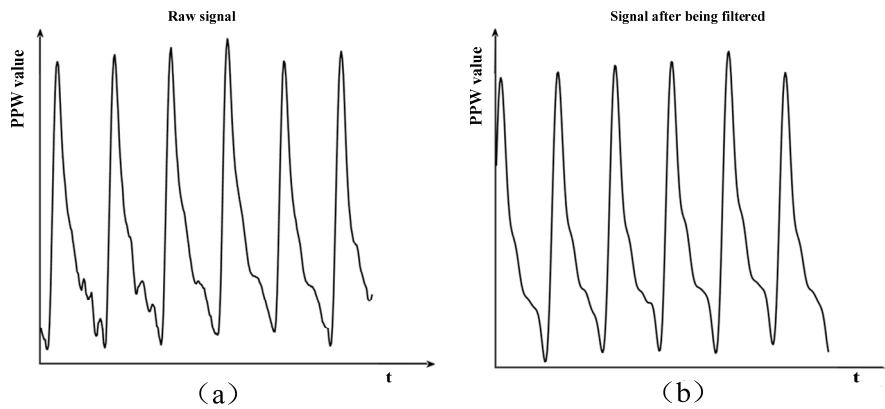


FIGURE 1. (a) Raw Signals (b) Signals after being filtered

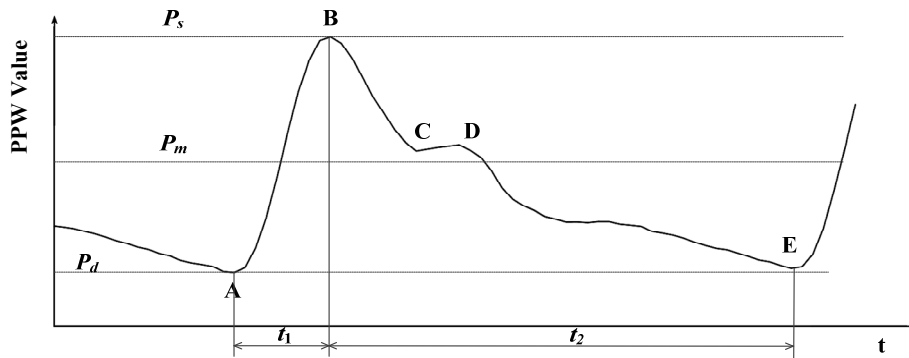


FIGURE 2. Time-domain signals of PPW in one cycle

Characteristics Extraction and Analysis

Some scholars find the best embedded dimension for their model's input data through experiments, which seems to be useful but lacks scientific foundation. As BP data is changing periodically and also affected by many physiological factors, extracting the characteristics of the PPW and selecting the most relevant ones as the input will be more scientific.

The conventional PPW time-domain signal in one cycle is shown in Fig. 2, in which some characteristic points are mainly composed of vertexes and the mathematical relationship between them[10]. The changes of these characteristic points on the curve reflect different physiological or pathological states of an organism. For example, Point A indicates that heart begins to contract and ejects blood to the aorta when the actual BP rises rapidly. Point B means the time that the contraction completes and the diastolic aorta is closing, with the BP reaching the maximum; what's more, the heart enters diastolic process after point B and finishes at point E, with two poles C and D. The amplitude of the waveform and the position of the poles are closely involved in the resistance and elasticity of blood vessels, and a cycle time T of PPW is related to the strength of the heart's pulsation function. Besides, the actual BP wave is similar to the PPW, but only SBP and DBP in each cycle were utilized in this paper. Notes that the SBP, the DBP and the characteristics are all from a same heart cycle.

Other characteristics of PPW also matters, like the maximum P_s , the minimum P_d , the average P_m , characteristic parameter k' , the pulse frequency HR, the time of duration in contraction t_1 , the time of duration in diastolic process t_2 , the average slope of ascent k , the output characteristic parameters of each beat Z , the ratio of the rising branch wave area to the total area of the waveform μ , some calculating methods are shown in Tab.2 and Fig 2.

k' reflects the physiological characteristics such as elasticity of blood vessel walls and blood viscosity in the cardiovascular system; HR mainly affects DBP. According to a large number of researchers, there is some correlation between BP and the periodic characteristics mentioned above, all of which were selected in this paper to analyze the

correlation factor with SBP and DBP respectively, and the most correlated ones would play a role of the input of LSTM-NN. 8 characteristics from 100 continuous cycles are shown in Fig 3, where the abscissa refers to the number of cycle. As we can see, most of them fluctuate with SBP and DBP.

And according to Pearson correlation formula (1), then the correlation coefficient between PPW characteristic parameters and SBP, DBP in one cycle was obtained, as shown in Table 3.

$$r = \frac{\sum_{i=1}^n (x_i - \bar{x})(y_i - \bar{y})}{\sqrt{\sum_{i=1}^n (x_i - \bar{x})^2 \sum_{i=1}^n (y_i - \bar{y})^2}} \quad (1)$$

Where ,the lengths of the sequence x and the sequence y are both n; \bar{x} and \bar{y} are the averages of two sequences, respectively; r is the correlation coefficient of the two sequences, with $|r| \leq 1.0$, and the closer to 1, the two sequences are more relevant.

TABLE 2. Calculating Methods of some PPW's characteristics

| Characteristic | Calculating Method | Unit |
|----------------|---|---------|
| k' | $k' = \frac{P_m - P_d}{P_s - P_d}$ | none |
| P_m | $P_m = \frac{\int_0^T p(t)dt}{T}$ | mmHg |
| k | $k = \frac{P_s}{t_1}$ | mmHg/ms |
| Z | $Z = P_s \cdot \left(1 + \frac{t_1}{t_2}\right)$ | mmHg |
| μ | $\mu = \frac{\int_0^{t_1} p(t)dt}{\int_0^T p(t)dt}$ | none |

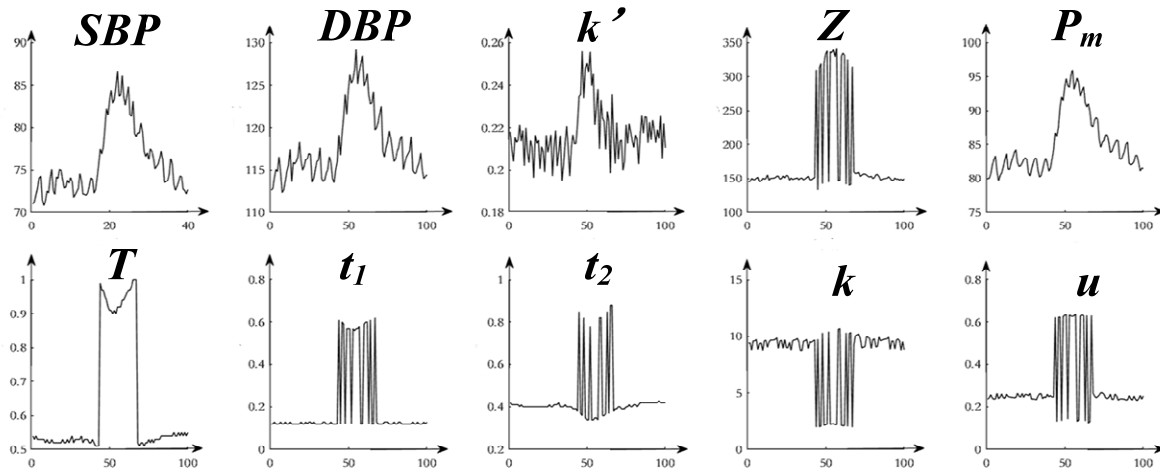


FIGURE 3. Oscillograms of each PPW signal's characteristic

TABLE 3. Correlation coefficients of PPW signal's characteristics with SBP and DBP respectively

| characteristic | k' | P_m | P_d | P_s | T | t_1 | t_2 | k | Z | μ |
|-----------------------------------|-------|-------|-------|-------|------|-------|-------|-------|------|-------|
| correlation coefficients with SBP | -0.53 | 0.99 | 0.98 | 1 | 0.35 | 0.62 | -0.11 | -0.08 | 0.61 | 0.44 |
| correlation coefficients with DBP | -0.51 | 0.98 | 1 | 0.98 | 0.36 | 0.61 | -0.12 | -0.10 | 0.63 | 0.45 |

ESTABLISHING THE COMPUTATION MODEL

With the clinical characteristic data above and signal processing theory, a short-term BP prediction model based on LSTM is established under the guidance of Deep Learning technology. The framework is shown in Figure 4. And this part focuses on how the LSTM model works.

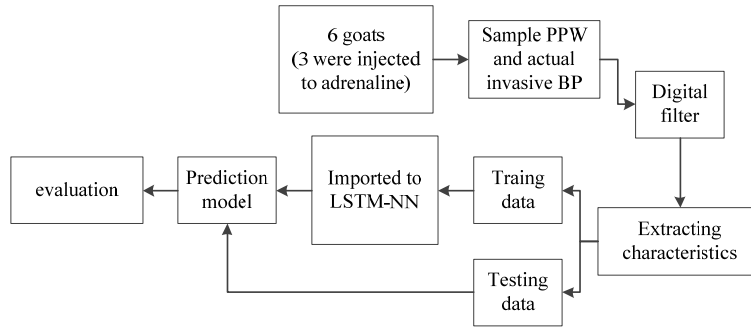


FIGURE 4. Frame of the blood pressure predicting model

Neural Network Model

As a perfect variant of RNN (Recurrent Neural Networks), LSTM-NN has been widely used in semantic recognition, machine translation, stock forecasting, wind farm wind speed prediction and other fields. In traditional artificial neural network (ANN), each hidden layer node is independent and there is no correlation between the output results. RNN has optimized it with ‘memory’ function, and the basic form of RNN is shown in Figure 5.

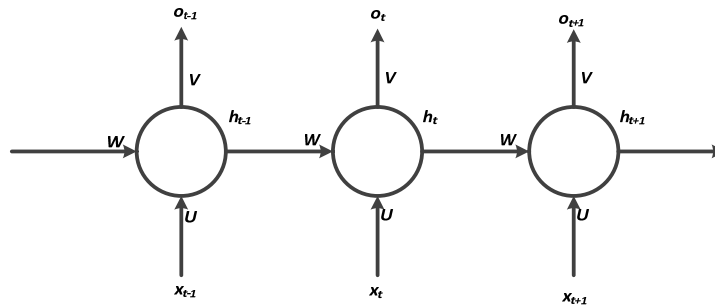


FIGURE 5. Fundamental form of RNN

x_t is the input sequence vector of RNN at time t, h is the state of the hidden layer, and O is the output vector. The weight matrix between the input layer and the hidden layer is U, the weight matrix between the hidden layer and the output layer is V, and the weight matrix between different moments of the same hidden layer is W. shown as (2)-(4):

$$a_t = b + Wh_{t-1} + Ux_t \quad (2)$$

$$h_t = \tanh(a_t) \quad (3)$$

$$o_t = c + Vh_t \quad (4)$$

Where b is the threshold matrix between the input layer and the hidden layer, and c is the threshold matrix between the hidden layer and the output layer.

Although RNN can shrink some training time due to parameter sharing, with the limited ability of memory in hidden layers, it is difficult to transmit information over long distances in RNN [11]. In order to solve the problems,

the LSTM first proposed by Sepp Hochreiter and Jurgen Schmidhunder in 1997 introduced three state gates and one ‘memory’ unit to filter the information based on RNN, which works more efficiently and especially the long-term time information can be utilized rationally. A unit structure of LSTM is shown in Figure 6. The ‘memories’ are divided into ‘long-term memory’ and ‘short-term memory’.

The three control gates are: 1. Input gate, to control the degree of inputting the long-term memory to the latest memory; 2. Forgetting gate, to forget some information selectively ; 3. Output gate, control the extent of impact caused by the short-term memory to the long-term memory. Its working principle is shown in equations (5)-(10):

$$C_t = f_t \times C_{t-1} + i_t \times \tilde{C}_t \quad (5)$$

$$f_t = \text{sigmoid}(W_{hf} \cdot h_{t-1} + W_{xf} \cdot x_t + b_f) \quad (6)$$

$$i_t = \text{sigmoid}(W_{hi} \cdot h_{t-1} + W_{xi} \cdot x_t + b_i) \quad (7)$$

$$\tilde{C}_t = \tanh(W_{hc} \cdot h_{t-1} + W_{xc} \cdot x_t + b_c) \quad (8)$$

$$h_t = o_t \times \tanh(C_t) \quad (9)$$

$$o_t = \text{sigmoid}(W_{ho} \cdot h_{t-1} + W_{xo} \cdot x_t + b_o) \quad (10)$$

Where W is the corresponding coefficient weight matrix, b is the bias vector, and f_t , i_t , o_t , and C_t are the calculation methods of the forgetting gate, the input gate, the output gate, and the memory unit, respectively, \tilde{C}_t means the latest memory.

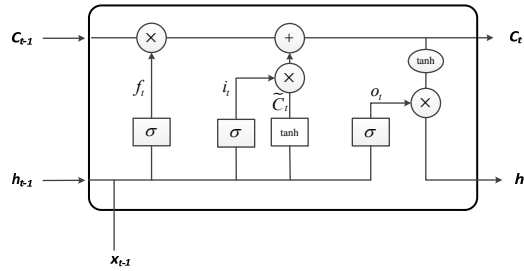


FIGURE 6. Structure of a LSTM-NN Cell

Short-term Blood Pressure Calculation Model Based On LSTM

Data Preprocessing

The ranges and dimensions of each characteristic are different from each other, so the accuracy of the prediction results will be seriously affected if input to the model directly. Therefore the data was normalized to [-1, 1] to eliminate the errors caused by dimensions, and finally the results should be mapped to the original ranges after prediction. The Normalized Fractal Method is used to standardize the data of each characteristics separately, and each sequence after normalized is in the range of [-1, 1], with all the preprocessed data obeys the Normal Distribution. The specific operation is as follows:

$$x_1(i) = \frac{x(i) - \bar{x}}{s(x)} \quad (11)$$

Where x is the original data sequence, x_1 is the normalized data sequence, and $s(x)$ is the standard deviation of sequence x.

Selecting Embedded Dimension

The main function of this model is to predict the actual SBP and DBP respectively with PPW signal, and in order to obtain the model we train it through some owed PPW data and corresponded SBP and DBP, with some to verify its accuracy.

For instance, when training the SBP (t) and DBP (t), we input $x(t), x(t - 1), \dots, x(t - m)$ to LSTM, but how to select m called embedded dimension to make the model work more efficient and to minimize the prediction error. Some scholars determine m by magnifying m from 1 gradually and observing prediction accuracy and iteration numbers, which lacks rigorous theoretical support. In this paper, autocorrelation analysis has been performed on the 6 PPW characteristic parameters, and the autocorrelation coefficient C of each parameter is calculated with lag coefficient ranging from 1 to 10, as shown in Table 4.

It can be seen from the results that the autocorrelation coefficients of P_m , P_d , and P_s are always higher than 90%, but C decreases When the lag hysteresis coefficient exceeds 8. And the autocorrelation coefficient of k' reaches its maximum at m is 6 and wanes after that, and t_1 and Z reach to their peaks when m is 7. Therefore, we choose the value of m is 7 as the embedded dimension of our BP prediction model. Namely, the input time-series x (t) and the output time-series y (t) are:

$$x(t) = \begin{Bmatrix} k'(t-6) & \dots & k'(t) \\ P_m(t-6) & \dots & P_m(t) \\ P_d(t-6) & \dots & P_d(t) \\ P_s(t-6) & \dots & P_s(t) \\ t_1(t-6) & \dots & t_1(t) \\ Z(t-6) & \dots & Z(t) \end{Bmatrix} \quad (12)$$

$$y(t) = \begin{Bmatrix} SBP(t+1) \\ DBP(t+1) \end{Bmatrix} \quad (13)$$

TABLE 4. Self-correlation coefficients of each characteristic under different embedding dimension

| Characteristics | | k' | P_m | P_d | P_s | t_1 | Z |
|---------------------|--|-------|-------|-------|-------|-------|-------|
| Embedding dimension | | | | | | | |
| 1 | | 0.576 | 0.982 | 0.983 | 0.961 | 0.514 | 0.591 |
| 2 | | 0.544 | 0.958 | 0.963 | 0.934 | 0.521 | 0.582 |
| 3 | | 0.561 | 0.947 | 0.957 | 0.925 | 0.594 | 0.643 |
| 4 | | 0.511 | 0.951 | 0.958 | 0.931 | 0.516 | 0.602 |
| 5 | | 0.502 | 0.963 | 0.967 | 0.901 | 0.525 | 0.586 |
| 6 | | 0.541 | 0.969 | 0.973 | 0.966 | 0.525 | 0.601 |
| 7 | | 0.493 | 0.949 | 0.959 | 0.931 | 0.596 | 0.667 |
| 8 | | 0.427 | 0.921 | 0.935 | 0.901 | 0.329 | 0.424 |
| 9 | | 0.414 | 0.903 | 0.924 | 0.886 | 0.337 | 0.416 |
| 10 | | 0.415 | 0.902 | 0.923 | 0.885 | 0.403 | 0.476 |

Selecting Parameters of LSTM Model

The functions of the model mainly are composed of network training and prediction. The number of input layers is 6 which should be equal to the embedded dimension obtained above, and the number of output layers is 2. According to the Kolmogorov theorem [12-15], the number of hidden layers is 5. And setting dropout probability is 0.2 to prevent over-fitting, which means making some nodes in hidden layer invalidated in each turn of training. What's more, Cross Entropy was employed to compute the Loss function in forward propagation, shown in formula (14), and Stochastic Gradient Descent Algorithm was imported to minimize the loss cost in training.

The initial learning rate is set to 0.9, and the batch_size is set to 15. The maximum number of training iterations is 300. On the other hand, BPTT algorithm was used to adjust the weights and thresholds in the backward propagation process.

$$loss = -\frac{1}{n} \cdot \sum_{i=1}^n (P^* \cdot \log(P + 0.01)) \quad (14)$$

Where P is the predicted value, P* is the actual value, N is the total number of predicted data, and a minimum error value of 0.01 is added to eliminate log (0).

EXPERIMENTS

All the characteristic data originated from the collected PPW data is divided into two groups: 75% (323 groups) for training model, and 25% (108 groups) for verification. Notes that the two groups of data are independent of each other in the time dimension without overlap. Training data is imported to the LSTM to get a desirable model capable to compute the corresponded DBP and SBP precisely, and testing data is to test the model. Compared with BP-NN, LSTM is more suitable and efficient. LSTM model is implemented in the Tensorflow Deep Learning framework and achieved via the Python programming language, and BP-NN runs in the MATLAB environment.

Evaluation Indexes of the Model

The Absolute Percentage Error (APE) and the Mean Relative Error (MRE) are selected to evaluate the accuracy of the prediction results, and the evaluation index S is used to estimate its robustness with the model performed for 100 times.

$$APE = \frac{|P-P^*|}{P^*} \times 100\% \quad (15)$$

$$MAPE = \frac{1}{N} \sqrt{\sum_{i=1}^N \left(\frac{|P-P^*|}{P^*}\right)^2} \times 100\% \quad (16)$$

$$S = \frac{n}{100} \times 100\% \quad (17)$$

Where P is the prediction value, P* is the actual value, N is the total number of prediction data, and n is the number of times when the error of the SBP and DBP are within the range of ± 4 mmHg.

Analyzing the Result

The parameters of the BP-NN are set as follows: the number of hidden layers is 5, the learning rate is 0.8, the activation functions of the hidden layer and the output layer are 'tansig' and 'pure-line' respectively, the Gradient Descent Algorithm works during training, and the maximum training turns is set to 5000, and the target error is 0.001. The prediction results of LSTM and BP-NN are shown in Fig. 7. The prediction results of the LSTM-NN model are more consistent with the actual values and are closer to the trend of the actual waveform, while the prediction results of the BP-NN are relatively poor. Making them work 100 times respectively to observe their robustness, the evaluation results are shown in Table 5. As it shows, the performance of the LSTM-NN is better than that of the BP-NN, indicating that LSTM-NN model has excellent robustness and can predict BP with 7 groups of PPW signal ahead precisely.

The SBP(t+1) and DBP(t+1) predicted by data x(t) directly without introducing the embedded dimension and being trained for 300 turns shows that the APE reaches to 5.85%, and MRE reaches to 3.75%, so it is feasible and critical to analyze the autocorrelation coefficient of the data before training to get the optimal embedded dimension.

TABLE 5. The comparison of prediction performances of BP neural network and LSTM model for diastolic and systolic pressures

| | LSTM | | | | BP | | | |
|-----|----------|------|-----------------------|-----|----------|-------|-----------------------|-----|
| | Max(APE) | MRE | Maximum errors (mmHg) | S | Max(APE) | MRE | Maximum errors (mmHg) | S |
| SBP | 1.01% | 0.3% | 1.05 | 98% | 3.8% | 1.07% | 4.3 | 68% |
| DBP | 3.05% | 0.6% | 1.8 | | 6% | 1.4% | 3.74 | |

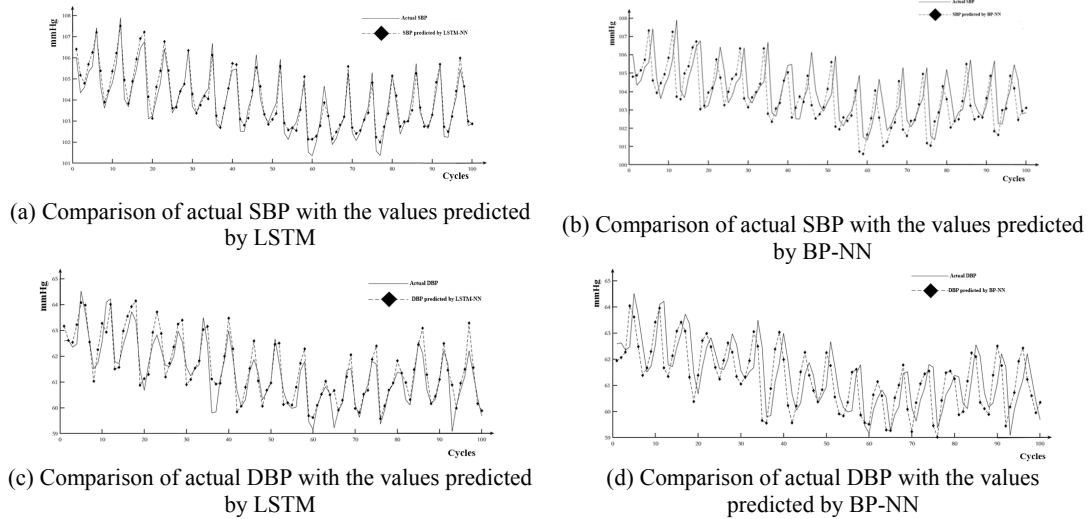


FIGURE 7. Predicting results of two models

CONCLUSION

First of all, we adopted scientific and rigorous animal experiments to collect the PPW signals and actual BP data of 6 adult goats under different conditions simultaneously. Then, the raw data was filtered and some clinical characteristics were extracted, and the characteristic parameters relevant to SBP and DBP were selected to compute their autocorrelation coefficient. The prediction result shows that LSTM has excellent robustness and accuracy when compared with BP-NN.

With deep combination between AI and biomedicine, large number novel portable physiological state measurement devices will appear, making it more efficient to prevent some diseases in advance.

ACKNOWLEDGEMENTS

This work was supported by the National Natural Science Foundation of China (81600394).

REFERENCES

1. Kuang Zeming, Huang Zhijun, Yuan Hong, et al. The value of dynamic blood pressure monitoring in the diagnosis and treatment of refractory hypertension [J], Chin J Hypertens, 2013, 21(9):728-730.
2. Chinese Hypertension League, ET, al. Chinese experts' agreements on the clinical application of dynamic blood pressure monitoring [J], Chin J Hypertens, 2015, 23(8):727-730.
3. Zhang Jinghui, Tang Hong, Research on prediction method of left ventricular blood pressure based on external heart sounds [J], Journal of Biomedical Engineering, 2017, 34(3): 335-341.
4. Enric Monte-Moreno. Non-invasive estimate of blood glucose and blood pressure from a
5. Photoplethysmograph by means of machine learning techniques [J], //Artificial Intelligence in Medicine, 2011, 53:127-138.

6. Qu Shihua, Wu Huawei, Qian Zhiyu, Li Weitao, ET, al. The improved algorithm of noninvasive blood pressure measurement based on characteristic parameters of pulse wave[J], Journal of Biomedical Engineering Research,2018,37(1):36-41.
7. Zhao Yanfeng, Yu Shuang, Wang Huiquan, et,al.Non - invasive measurement of continuous blood pressure based on pulse transit time and pulse wave characteristic parameters[J], Journal of Biomedical Engineering Research.2018, 37(1):42-45.
8. Shu Fan, Qu Dan, Zhang Wenlin, ET, al. A Speech Recognition Method Using Long Short-Term Memory Network in Low Resources[J], JOURNAL OF XI'AN JIAOTONU UNIVERSITY,2017,51(10):120-127.
9. Zhang Yuhang, Qiu Caiming, He Xing, ET, al. A short - term load forecasting method based on LSTM neural network[J], Electric Power Information and Communication Technology,2017,15(9):19-25.
10. Frank P.-W. Lo, Charles X.-T. Li, Jiankun Wang,et,al. Continuous Systolic and Diastolic Blood Pressure Estimation utilizing Long Short-term Memory Network[C].//Annual International Conference of the IEEE Engineering in Medicine and Biology Society,2017,10(1109):1853-1856.
11. Luo Zhichang, Zhang Song, Yang Yimin. Engineering Analysis for Pulse Wave and its Application in Clinical Practice [M], Science Press, 2006:21.
12. Wang Chen, Hu Zhenbang, GAO Jie. The Principles of Deep Learning and Application of Tensorflow [M], Publishing House of Electronics Industry, 2017:139.
13. Belabbes Richard G. On Using SVM and Kolmogorov Complexity for spam Filtering[C].//FLAIRS Conference.2008:130-135
14. Nikvand N, Wang Z. Generic image similarity based on Kolmogorov complexity[C], //2010 17th IEEE International Conference on Image Processing(IC:IP). IEEE, 2010: 309-312.
15. Tao Xiaolei. Study of Kolmogorov Complexity Based Clustering Algorithms [D]. Nanjing University of Aeronautics and Astronautics, 2013.
16. Ukil A. Application of Kolmogorov complexity detection[C].//2010 16th Asia-Pacific Conference on Communications (APCC).IEEE, 2010: 141-146.